



ACADEMIC  
PRESS

Available online at [www.sciencedirect.com](http://www.sciencedirect.com)

SCIENCE @ DIRECT®

Journal of Solid State Chemistry 171 (2003) 189–194

JOURNAL OF  
SOLID STATE  
CHEMISTRY

<http://elsevier.com/locate/jssc>

# Synthesis and luminescent properties of supramolecules of $\beta$ -diketonate of Eu(III) and crown ethers as ligands

Maria Claudia F.C. Felinto,<sup>a,\*</sup> Claudia S. Tomiyama,<sup>a</sup> Hermi F. Brito,<sup>b</sup> Ercules E.S. Teotonio,<sup>b</sup> and Oscar L. Malta<sup>c</sup>

<sup>a</sup>Centro de Química e Meio Ambiente Instituto de Pesquisas Energéticas e Nucleares C.P. 26077, C.E.P.05508-970 São Paulo SP, Brazil

<sup>b</sup>Departamento de Química Fundamental Instituto de Química da Universidade de São Paulo C.P. 26077, C.E.P.05508-970 São Paulo SP, Brazil

<sup>c</sup>Departamento de Química Fundamental UFPE CCEN Cidade Universitária C.E.P.50670-901 Recife PE, Brazil

Received 6 June 2002; received in revised form 1 August 2002; accepted 17 November 2002

## Abstract

This work reports the synthesis and luminescence behavior of the diaquatris(thenoyltrifluoroacetate)europium(III) with dibenzo18-crown-6 (DB18C6) and 18-crown-6 (18C6), in the solid state. The new compounds  $\text{Eu}(\text{TTA})_3(\text{H}_2\text{O})_2(\text{DB18C6})_2$  and  $\text{Eu}(\text{TTA})_3(\text{H}_2\text{O})_2(18\text{C6})_2$  were characterized by elemental analysis, infrared spectroscopy, thermal analysis and scattering electronic microscopy. The emission spectra show narrow emission bands that arise from the  ${}^5\text{D}_0 \rightarrow {}^7\text{F}_J$  transitions ( $J = 0-4$ ) of the  $\text{Eu}^{3+}$  ion. The spectral data of the  $\text{Eu}(\text{TTA})_3(\text{H}_2\text{O})_2(\text{DB18C6})_2$  and  $\text{Eu}(\text{TTA})_3(\text{H}_2\text{O})_2(18\text{C6})_2$  compounds present, respectively, one and two peaks assigned to the  ${}^5\text{D}_0 \rightarrow {}^7\text{F}_0$  transition ( $\sim 578$  nm), suggesting one and two sites of symmetry around the metal ion. In addition, the luminescence decay curves of these DB18C6 and 18C6 systems were better fitted by a mono- and bi-exponential decays, respectively. The values of the experimental intensity parameters ( $\Omega_2$ ) indicate that the europium ion in the complexes is in a highly polarizable chemical environment. The values of emission quantum efficiencies for the two Eu(III)-supramolecular compounds are similar ( $\eta = 26\%$ ).

© 2003 Elsevier Science (USA). All rights reserved.

**Keywords:** Supramolecular compounds; Crown ethers; Europium; Luminescence; Thenoyltrifluoroacetate

## 1. Introduction

The design of complexes of the trivalent rare earth ions, RE(III), with encapsulated ligands is an important subject in the supramolecular field due to the possibility to obtain stable luminescent compounds. An important aspect of this research consists in the possibility to optimize the luminescence properties of the metal ion by a suitable selection of ligands [1,2]. Among the investigated macrocyclic ligands, dibenzo18-crown-6 (DB18C6) and 18-crown-6 (18C6) have been used for determination of ultra-trace amount of europium in high-purity lanthanum, praseodymium and dysprosium oxides [3]. Besides, this kind of ligands proved to be useful in demonstrating the extreme sensitivity of the Eu(III) ion as a luminescent probe [4]. Photoluminescent studies of rare earth complexes with macrocyclic ligands

have been studied extensively in the last years [3–5]. In order to optimize the emission quantum yield of a light conversion molecular device (LCMD) several processes must be controlled: (i) the ligand absorption and internal decay processes, (ii) the efficiency of the ligand-to-metal energy transfer and (iii) the luminescence efficiency of the metal ion.

Based on the luminescence properties of RE compounds, mainly the Eu(III), Tb(III) and Sm(III) ions have been potentially used as fluorescent sensors in natural, medical, analytical and bioinorganic sciences [6]. These ions possess long lifetime of the emitting states and exhibit sharp emission lines in the visible region. The Eu(III) ion usually presents emission spectra with narrow bands corresponding to the  ${}^5\text{D}_0 \rightarrow {}^7\text{F}_J$  transitions (where  $J = 0-4$ ) and a great advantage is that the  ${}^5\text{D}_0 \rightarrow {}^7\text{F}_0$  transition is non-degenerate, and can be used to indicate if the Eu(III) ion occupies only one or more than one symmetry site belonging to the  $C_s$ ,  $C_n$  or  $C_{nv}$  point groups. The other facility to work with this ion is

\*Corresponding author. Fax: +55-11-3816-9325.

E-mail address: [mfelinto@net.ipen.br](mailto:mfelinto@net.ipen.br) (M.C.F.C. Felinto).

that the intensity of the  $^5D_0 \rightarrow ^7F_1$  transition is not much influenced by a change in the surroundings of the metal ion, since it is allowed by magnetic dipole and consequently it can be used as a reference transition [7].

The RE(III) ions have particular affinity to coordinate to organic molecules containing oxygen, nitrogen or sulfur as donor atoms, with the following binding preference:  $O > N > S$  [8]. These donor atoms are frequently found in biochemical systems which explains the number of recent studies involving RE(III) complexes with molecules biologically important [6]. Thus, crown ether compounds are capable of encapsulating rare earth ions giving rise to stable complexes in solution and can play the role of “antenna” [4].

This paper reports the characterization and luminescence investigation of new Eu(III)- $\beta$ -diketonate compounds with crown ether ligands. The present study is dedicated to the influence of the 18C6 and DB18C6 ligands on the photoluminescence properties and energy transfer processes in these compounds. In addition, the Eu-supermolecules interaction has been studied via electronic spectroscopy based on the intensity parameters ( $\Omega_\lambda$ ), emission quantum efficiency ( $\eta$ ) and the lifetime of the emitting  $^5D_0$  level.

## 2. Experimental section

Crystals of the  $[\text{Eu}(\text{TТА})_3 \cdot (\text{H}_2\text{O})_2]$  complex were synthesized as described in the literature by Charles and Ohlmann [9] with a slight modification of the method where pentane was used instead of petroleum ether to remove the excess of chelating agent [10].

The precursor complex and crown ether ligands were dissolved separately in ethanol and mixed under stirring until the formation of a yellow precipitate. The powders formed were washed with ethanol to eliminate the hydrated complex and ligand excess. The solid compounds were dried under vacuum over silica in a desiccator.

The carbon and hydrogen contents were determined by usual microanalytical procedures using a Perkin-Elmer microelemental analyzer (Model 2400). The percentage of Eu(III) was determined by complexometric titration with EDTA [11]. The infrared spectra were measured at room temperature in a Bomem MD 102 spectrometer in the spectral range of  $4000\text{--}400\text{ cm}^{-1}$ . It was applied nujol mull suspension techniques in obtaining the infrared spectra of the compounds and free ligands. The scattering electronic microscopy (SEM) was obtained in a microscope Philips XR-30 using a sputtering technique with gold as covering material. Differential thermogravimetric analyses (DTA) were performed in a NETZSCH STA 409C using aluminum crucibles with  $\sim 18.40\text{ mg}$  of sample, under dynamic synthetic air atmosphere ( $40\text{ mL min}^{-1}$ )

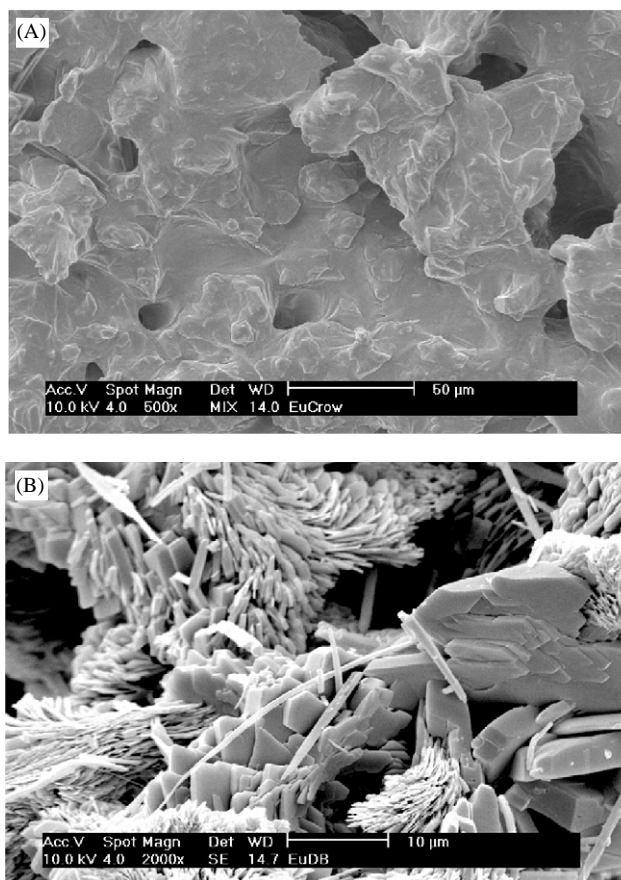


Fig. 1. SEM of the  $[\text{Eu}(\text{TТА})_3 \cdot (\text{H}_2\text{O})_2\text{L}_2]$  compounds, where  $L = 18\text{C}6$  (A) and  $\text{DB}18\text{C}6$  (B).

and heating rate of  $15^\circ\text{C min}^{-1}$  in the temperature interval of  $20\text{--}1000^\circ\text{C}$ . The thermogravimetric (TG) curves were recorded with a thermobalance model NETZSCH STA 409C in the temperature interval of  $20\text{--}1000^\circ\text{C}$ , using platinum aluminum with  $\sim 18.0\text{ mg}$  of sample, under dynamic synthetic air atmosphere ( $40\text{ mL min}^{-1}$ ) and heating rate of  $15^\circ\text{C min}^{-1}$ .

The excitation and emission spectra of the powdered samples were performed in a SPEX Fluorolog-2 spectrofluorimeter, model FL212 system, double grating  $0.22\text{ m}$  SPEX 1680 monochromator, and a  $450\text{ W}$  Xenon lamp as excitation source using the front face mode. This apparatus was fully controlled by a DM3000F spectroscopic program and computer. The lifetime data of the supermolecule compounds were recorded at room temperature, using a phosphorimeter (SPEX 1934D) accessory coupled to the spectrofluorometer. The decay curves were recorded monitoring the hypersensitive  $^5D_0 \rightarrow ^7F_2$  transition of the Eu (III) ion.

## 3. Results and discussion

The C, H and Eu(III) contents found/calculated for the supermolecular compounds with the ligands are:

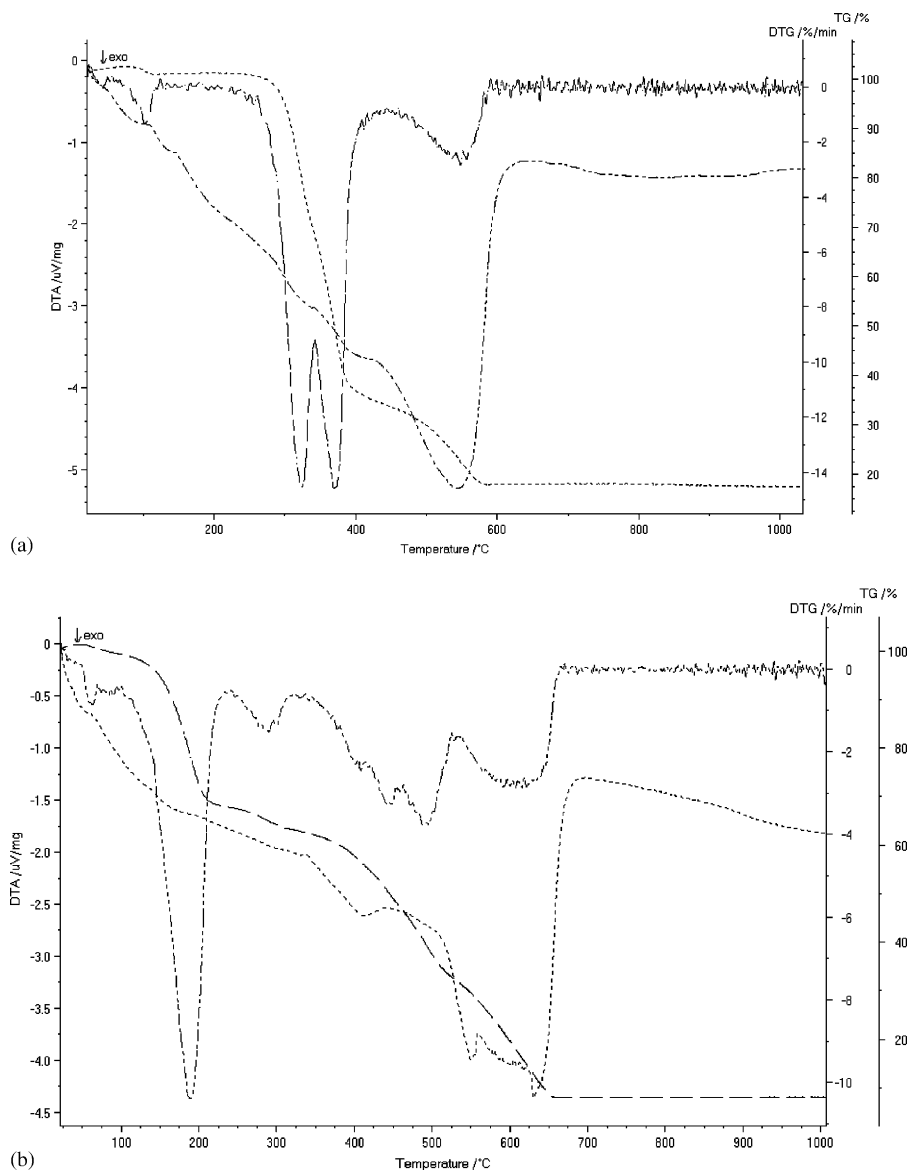


Fig. 2. TG and DTA curves of the  $[\text{Eu}(\text{TTA})_3 \cdot (\text{H}_2\text{O})_2\text{L}_2]$  compounds, where  $L = 18\text{C}6$  (A) and  $\text{DB}18\text{C}6$  (B).

18C6 (C: 41.69/41.18; H: 4.59/4.60 and Eu(III): 13.60/13.52) and DB18C6 (C: 48.80/48.36 H: 4.80/4.2 and Eu(III): 9.75/9.65) these data agree with the following formula  $\text{Eu}(\text{TTA})_3(\text{H}_2\text{O})_2(18\text{C}6)_2$  and  $\text{Eu}(\text{TTA})_3(\text{H}_2\text{O})_2(\text{DB}18\text{C}6)_2$ .

The infrared (IR) spectra show a displacement of  $\nu(\text{C}=\text{O})$  stretching mode from  $\sim 1680\text{ cm}^{-1}$ , in free TTA, to approximately  $1600\text{ cm}^{-1}$  in the compounds, indicating that the metal ion is coordinated through the oxygen atoms [12,13]. A precise assignment of the  $\nu_{\text{as}}(\text{C}-\text{O}-\text{C})$  and  $\nu_{\text{s}}(\text{C}-\text{O}-\text{C})$  stretching vibrational modes around  $1100\text{ cm}^{-1}$  is difficult due to the fact that the TTA vibrational transitions ( $\nu_{\text{as}}\text{C}-\text{F}_3$ ,  $\nu_{\text{s}}\text{C}-\text{F}_3$  and  $\nu\text{C}-\text{F}$ ) mask these bands [12]. The IR spectra of the crown ether compounds as compared to that of the  $[\text{Eu}(\text{TTA})_3(\text{H}_2\text{O})_2]$  compound (figure not shown) also

present a broad band at  $3396\text{ cm}^{-1}$  which is attributed to  $\nu(\text{O}-\text{H})$  stretching, confirming that the supermolecules were isolated in the hydrated form.

Fig. 1 shows the agglomerated structures of the crown ether compounds. For the supermolecule  $\text{Eu}(\text{TTA})_3(\text{H}_2\text{O})_2(18\text{C}6)_2$ , the formation of two phases is observed, one of them behaving like a film recovering the other, while for the  $\text{Eu}(\text{TTA})_3(\text{H}_2\text{O})_2(\text{DB}18\text{C}6)_2$  compound the agglomerate presents non-homogeneous morphology, as suggested by the layers formed.

Fig. 2 exhibits the DTA/TG/DTG curves in the temperature range from 20 to  $1000^\circ\text{C}$  for the  $\text{Eu}(\text{TTA})_3(\text{H}_2\text{O})_2(18\text{C}6)_2$  and  $\text{Eu}(\text{TTA})_3(\text{H}_2\text{O})_2(\text{DB}18\text{C}6)_2$  supermolecules. The DTA curve of the supermolecules presents a single broad exothermic peak assigned to thermal decomposition. The DTG and TG curves

present events relative to water loss, in the interval of 20–200°C, indicating that these new compounds are in hydrated form. This is corroborated by microanalytical procedures and IR spectroscopy. The DTG and TG curves also show that the profile of the weight loss stages is not very well defined, reflecting the complexity of the thermal decomposition reactions that are occurring in these systems.

The excitation spectra of the Eu(III)-supermolecules, recorded in the 250–570 nm spectral range by monitoring the emission at the hypersensitive  $^5D_0 \rightarrow ^7F_2$  transition are presented in Fig. 3. The spectral data of  $\text{Eu}(\text{TTA})_3(\text{H}_2\text{O})_2(\text{DB18C6})_2$  exhibit two broad bands corresponding to the ligands and also present narrow lines assigned to the Eu(III) ion transitions:  $^7F_0 \rightarrow ^5D_2$  at 463 nm and  $^7F_0 \rightarrow ^5D_1$  at 524, 533 and 539 nm, while for  $\text{Eu}(\text{TTA})_3(\text{H}_2\text{O})_2(18\text{C6})_2$  the observed transitions are:  $^7F_0 \rightarrow ^5D_2$  at 464 nm and  $^7F_0 \rightarrow ^5D_1$  at 525 and 534 nm.

The emission spectra were recorded in the range of 520–580 nm (Fig. 4A) and from 580 to 720 nm (Fig. 4B) under excitation around 394 nm, at 77 K. The spectrum of  $\text{Eu}(\text{TTA})_3(\text{H}_2\text{O})_2(\text{DB18C6})_2$  shows the  $^5D_0 \rightarrow ^7F_J$  transitions containing  $(2J + 1)$ -components, suggesting the presence of only one site symmetry for the Eu(III) ion (Table 1). On the other hand, the spectrum of  $\text{Eu}(\text{TTA})_3(\text{H}_2\text{O})_2(18\text{C6})_2$  presents two peaks for the  $^5D_0 \rightarrow ^7F_0$  transition, indicating the presence of different chemical environments around the Eu(III) ion. This is confirmed by the fact that all the  $^5D_0 \rightarrow ^7F_J$  transitions, for this compound, present more than  $2J + 1$  components. In the luminescence spectra no broad band in the 500–560 nm region, assigned to triplet states of the TTA chelate, are observed. This shows an efficient energy transfer from the lowest TTA triplet state to the emitting  $^5D_0$  level of the Eu(III) ion [2].

The experimental intensity parameters,  $\Omega_2$  and  $\Omega_4$ , were determined from the emission spectra (Fig. 3) based on the  $^5D_0 \rightarrow ^7F_2$  and  $^5D_0 \rightarrow ^7F_4$  electronic transitions of the Eu(III) ion, and they are estimated according to the following equation [14]:

$$A_{0J} = \frac{4e^2\omega^3}{3hc^3} \chi \sum_{\lambda} \Omega_{\lambda} \langle ^7F_J || U^{(\lambda)} || ^5D_0 \rangle^2, \quad (1)$$

where,  $\lambda = 2$  and 4,  $A_{0J}$  is the coefficient of spontaneous emission,  $\chi$  is the Lorentz local field correction term that is given by  $n(n^2 + 2)^2/9$  with a refraction index  $n = 1.5$ , and  $\langle ^7F_J || U^{(\lambda)} || ^5D_0 \rangle^2$  are the squared reduced matrix elements whose values are 0.0032 and 0.0023 for  $J = 2$  and 4, respectively. The experimental coefficients of spontaneous emission,  $A$ , to be used in Eq. (1) are obtained according to the relation  $A_{0J} = A_{01}(I_{0J}/I_{01})(\nu_{01}/\nu_{0J})$ , where  $I_{01}$  and  $I_{0J}$  are the integrated intensities of the  $^5D_0 \rightarrow ^7F_1$  and  $^5D_0 \rightarrow ^7F_J$  transitions ( $J = 2$  and 4) with  $\nu_{01}$  and  $\nu_{0J}$  being the

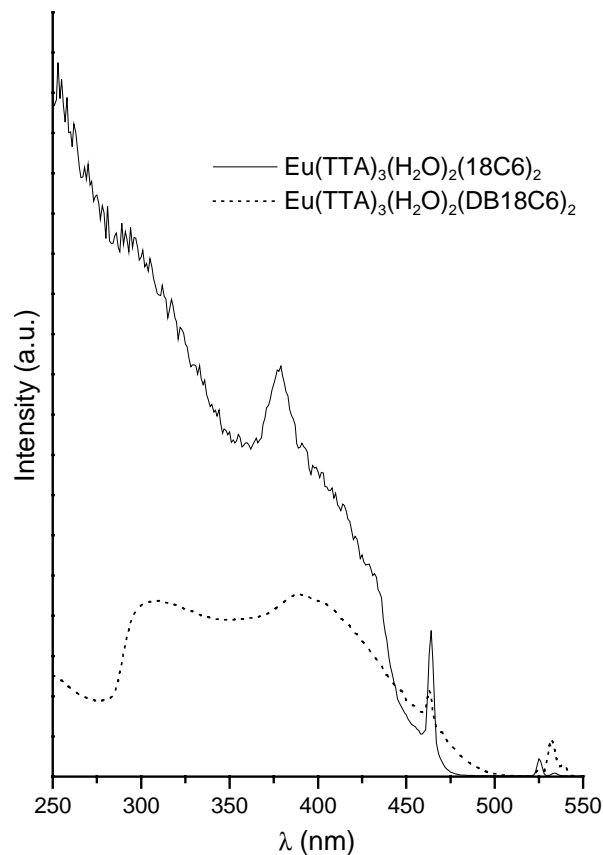


Fig. 3. Excitation spectra of the  $[\text{Eu}(\text{TTA})_3 \cdot (\text{H}_2\text{O})_2 L_2]$  compounds, where  $L = 18\text{C6}$  (solid line) and  $\text{DB18C6}$  (dotted line), with emission monitored at 612 nm, at room temperature.

respective energy barycenters of these transitions. The coefficient of spontaneous emission,  $A_{01}$ , is given by the expression  $A_{01} = 0.31 \times 10^{-11} (n^3 (\nu_{01})^3)$  [2].

The intensity parameters, particularly  $\Omega_2$ , are sensitive to changes in the chemical environment around the Eu(III) ion. The values of  $\Omega_2$  and  $\Omega_4$  for the Eu(III)-supermolecules and hydrated compound are presented in Table 2. It is noted that the hydrated compound has a value of  $\Omega_2$  higher than those determined for both Eu(III)-supermolecules, suggesting the smaller hypersensitive behavior of the  $^5D_0 \rightarrow ^7F_2$  transition in these new compounds and a lower covalent character of the interaction between the Eu(III) ion and the oxygen ligating atoms. As a consequence, this might also suggest that the chelate effect of TTA (bidentate ligand) is perturbed by the addition of crown ether molecules in the first coordination sphere of the europium ion, conferring a smaller electric dipole character to the  $^5D_0 \rightarrow ^7F_2$  transition. However, when we compare the values of the  $\Omega_2$  parameter determined for the Eu-macrocyclic compounds in this work with those reported in Ref. [13] it is possible to establish the following series:  $\text{YX}(\text{15C5})_2 > \text{YX}(\text{DCH18C6})_2 > \text{Y}(\text{DCH18C6}) > \text{YX}_2(\text{15C5}) > \text{YX}_2 > \text{YX}_2(\text{DB18C6})_2 > \text{YX}_2(\text{18C6})_2$ , where  $Y = \text{Eu}(\text{TTA})_3$  and  $X = \text{H}_2\text{O}$ .



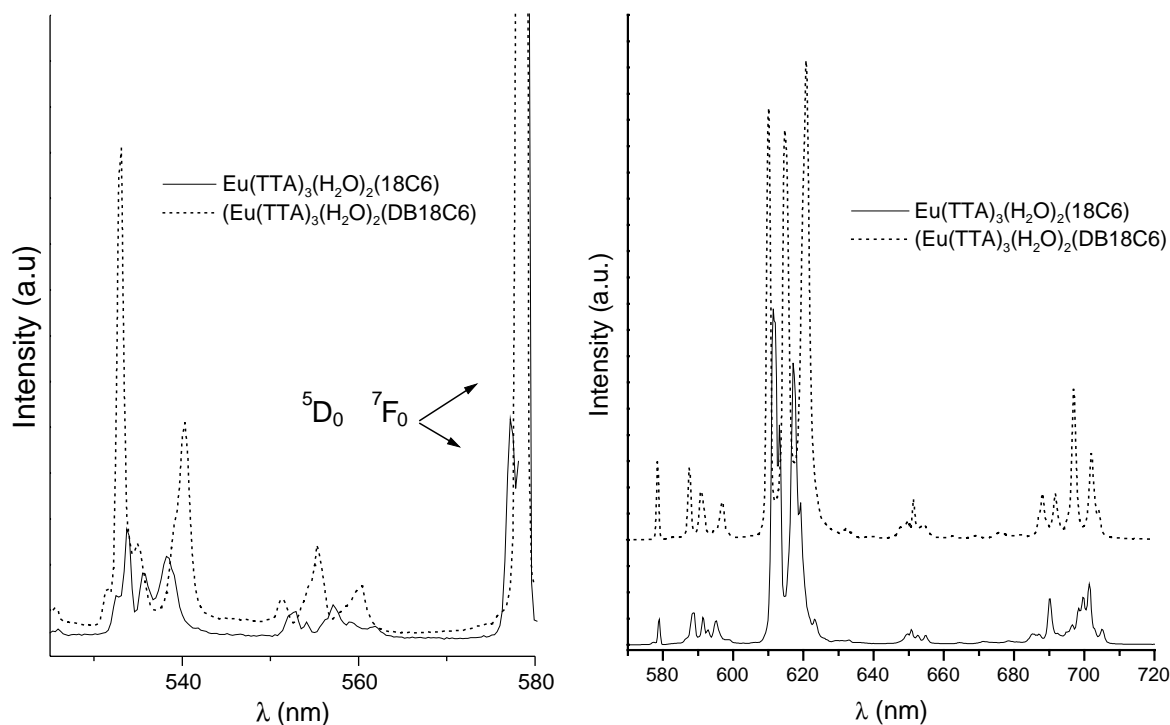


Fig. 4. Emission spectra of the  $[\text{Eu}(\text{TTA})_3 \cdot (\text{H}_2\text{O})_2 \text{L}_2]$  compounds, where  $L = 18\text{C6}$  (solid line) and  $\text{DB18C6}$  (dotted line), under excitation at 394 nm, at 77 K. (A) Amplified spectra recorded in the range of 520–580 nm, and (B) spectral range from 560 to 720 nm.

Table 1

Energy levels of the  ${}^5\text{D}_{0,1} \rightarrow {}^7\text{F}_{0-4}$  transitions ( $\text{cm}^{-1}$ ) observed in the emission spectra of the  $[\text{Eu}(\text{TTA})_3 \cdot (\text{H}_2\text{O})_2]$  and  $[\text{Eu}(\text{TTA})_3 \cdot (\text{H}_2\text{O})_2 \text{L}_2]$  compounds, where  $L = 18\text{C6}$  and  $\text{DB18C6}$

Transitions	$\text{H}_2\text{O}$	18C6	DB18C6
${}^5\text{D}_1 \rightarrow {}^7\text{F}_0$	—	19015	19024
${}^5\text{D}_1 \rightarrow {}^7\text{F}_1$	—	18878, 18732 18674, 18580	18809, 18763 18692, 18549 18508
${}^5\text{D}_1 \rightarrow {}^7\text{F}_2$	—	18086, 18084 17979, 17950 17882, 17797	18136 17998 17843
${}^5\text{D}_0 \rightarrow {}^7\text{F}_0$	17268	17323, 17271	17289
${}^5\text{D}_0 \rightarrow {}^7\text{F}_1$	16984 16906 16793	17050, 16990 16912, 16892 16801, 16692	17024 16929 16750
${}^5\text{D}_0 \rightarrow {}^7\text{F}_2$	16369, 16279 16221, 16149 16097	16356, 16340 16308, 16205 16150, 16041	16396 16206 16103
${}^5\text{D}_0 \rightarrow {}^7\text{F}_4$	14514 14497 14249 14221 14163	14742, 14594 14556, 14486 14442, 14355 14318, 14288 14257, 14184	14531 14455 14343 14245 14203 - -

Table 2 also presents the  $\Omega_4$  value of the precursor hydrated complex that is about twice smaller than for the  $\text{Eu}(\text{TTA})_3(\text{H}_2\text{O})_2(\text{DB18C6})_2$  and  $\text{Eu}(\text{TTA})_3(\text{H}_2\text{O})_2(18\text{C6})_2$  compounds, indicating a perturbation on the chelate effect of the bidentate TTA by steric factors from the crown ether ligands.

From the luminescence decay curves for the supermolecules we have determined the lifetime values (Table 2) of the emitting  ${}^5\text{D}_0$  level at room temperature. These curves were fitted with a mono- and bi-exponential curves for the compounds with  $\text{DB18C6}$  and  $18\text{C6}$  ligands, respectively.

In Table 2 the lifetimes of the emitting  ${}^5\text{D}_0$  level in the  $\text{Eu}(\text{III})$ -macromolecules are not very different from the value in the hydrated complex. The rather short lifetime values in these three cases is due to the non-radiative decay channels associated to the vibronic coupling with the  $\text{H}_2\text{O}$  molecules and  $\text{CH}$  of the crown ether.

The lifetime, non-radiative ( $A_{\text{nrad}}$ ) and radiative ( $A_{\text{rad}}$ ) rates are related through the equation  $A_{\text{tot}} = 1/\tau = A_{\text{rad}} + A_{\text{nrad}}$ . The radiative ( $A_{\text{rad}}$ ) rates were obtained by summing over the radiative rates  $A_{0J}$  for each  ${}^5\text{D}_0 \rightarrow {}^7\text{F}_J$  transition ( $\sum_J A_{0J}$ ). The quantum efficiencies of the emitting  ${}^5\text{D}_0$  level were obtained from the ratio  $\eta = A_{\text{rad}}/(A_{\text{rad}} + A_{\text{nrad}})$ .

The  $\text{Eu}(\text{III})$ -supermolecules exhibit the same emission quantum efficiencies ( $\eta = 26\%$ ), and they are quite close to the value for the hydrated complex ( $\eta = 29\%$ ). Again this is due to the presence of  $\text{O-H}$  and  $\text{C-H}$  oscillators

Table 2

Experimental intensity parameters ( $\Omega_2$ ), radiative ( $A_{\text{rad}}$ ) and non-radiative ( $A_{\text{nrad}}$ ) decay rates, lifetime of the emitting level and emission quantum efficiency ( $\eta$ ) of the  $[\text{Eu}(\text{TTA})_3 \cdot (\text{H}_2\text{O})_2]$  and  $[\text{Eu}(\text{TTA})_3 \cdot (\text{H}_2\text{O})_2 L_2]$  compounds, where  $L = 18\text{C}6$  and  $\text{DB18C}6$

Ligands	$\Omega_2 \times 10^{20}$ (cm <sup>2</sup> )	$\Omega_4 \times 10^{20}$ (cm <sup>2</sup> )	$A_{\text{rad}}$ (s <sup>-1</sup> )	$A_{\text{nrad}}$ (s <sup>-1</sup> )	$A_{\text{tot}}$ (s <sup>-1</sup> )	$R_{02}$	$\tau$ (ms)	$\eta$ (%)
H <sub>2</sub> O	33.0	4.6	1110	2736	3846	0.013	0.260	29
18C6	20.0	11.1	834.9	2419	3254	0.013	0.305–1.002	26
DB18C6	31.0	11.6	1155	3345	4500	0.017	0.222	26

in both systems, which effectively quench the luminescence. This is corroborated by comparison with the  $[\text{Eu}(\text{TTA})_3(\text{DBSO})_2]$  complex in solid state, which has a very high quantum efficiency ( $\eta = 85\%$ ) [15–18].

#### 4. Conclusions

The emission spectrum of the DB18C6 system shows only one peak for the  $^5\text{D}_0 \rightarrow ^7\text{F}_0$  transition indicating the presence of a single chemical environment around the Eu(III) ion. In contrast, the 18C6 system presents two sites of symmetry for the  $\text{Eu}^{3+}$  ion. The DB18C6 system has a smaller value of the  $\Omega_2$  parameter as compared with the hydrated precursor complex, suggesting a lower covalent character of the interaction between the Eu(III) ion and the oxygen ligating atoms. The Eu(III)-supermolecules present the same emission quantum efficiencies. Furthermore, these values are similar to the value of the hydrated complex, and this fact is due to luminescence quenching produced by coupling with OH and CH vibrations. Finally, the above results suggest that the Eu(III) supermolecules are promising photochemically stable compounds to be used as luminescent probes in the DNA hybridization, protein assay, and provide clear evidence of the usefulness of this type of study in the development of new rare earth sensitizers and probes.

#### Acknowledgments

The authors are grateful to the Conselho Nacional de Desenvolvimento Científico e Tecnológico (CNPq-RE-NAMI) and the Fundação de Amparo à Pesquisa do Estado de São Paulo (FAPESP) for financial support. We also acknowledge the LMEV-IPEN by the SEM.

#### References

- [1] N. Sabbatini, M. Guardigli, J.M. Lehn, *Coord. Chem. Rev.* 123 (1993) 201–247.
- [2] G.F. de Sá, O.L. Malta, C.M. Donegá, A.M. Simas, R.L. Longo, P.A. Santa-Cruz, E.F. da Silva Jr., *Coord. Chem. Rev.* 196 (2000) 165–195.
- [3] N.M. Sita, T.P. Rao, C.S.P. Iyer, A.D. Damadara, *Talanta* 44 (1997) 423–426.
- [4] J.-C.G. Bünzli, G.R. Choppin (Eds.), *Lanthanide Probes in Life, Chemical and Earth Sciences: Theory and Practice*, Elsevier, Amsterdam, 1989, pp. 219–270.
- [5] J.-C.G. Bünzli, N. André, N. Alhabiri, G. Muller, C. Piguet, *J. Alloy Compd.* 303–304 (2000) 66–74.
- [6] I. Hemillä, T. Stahlberg, P. Mottram (Eds.), *Bioanalytical Applications of Labelling Technologies*, Wallac Oy, Turku, 1994, pp. 145–242.
- [7] G. Blasse, B.C. Grabmaier, *Luminescent Materials*, Springer, Heidelberg, 1994.
- [8] F.S. Richardson, *Chem. Rev.* 82 (1982) 541–552.
- [9] R.G. Charles, R.C. Ohlmann, *J. Inorg. Nucl. Chem.* 27 (1965) 255–259.
- [10] H.F. Brito, O.L. Malta, C.A.A. Carvalho, J.F.S. Menezes, L.R. Souza, R. Ferraz, *J. Alloy Compd.* 275–277 (1998) 254–257.
- [11] S.J. Lyle, M.M. Rahman, *Talanta* 10 (1963) 1177–1182.
- [12] K. Nakamoto, *Infrared and Raman Spectra of Inorganic and Coordination Compounds*, Wiley-Interscience Publication, New York, 1986, pp. 90–101.
- [13] H.F. Brito, O.L. Malta, L.R. Souza, J.F.S. Menezes, C.A.A. Carvalho, *J. Non-Cryst. Solids* 247 (1999) 129–133.
- [14] B.R. Judd, *Phys. Rev.* 127 (1962) 750–761.
- [15] W.T. Carnall, H. Crosswhite, H.M. Crosswhite, *Energy Level Structure and Transition Probabilities of the Trivalent Lanthanides in LaF<sub>3</sub>*, Argonne National Laboratory Report, unnumbered, 1977.
- [16] O.L. Malta, H.F. Brito, J.F.S. Menezes, F.R.G. Silva, S. Alves Jr., F.S. Farias Jr., A.V.M. de Andrade, *J. Lumin.* 75 (1997) 255–268.
- [17] O.L. Malta, H.F. Brito, J.F.S. Menezes, F.R.G. Silva, C.M. Donegá, S. Alves Jr., *Chem. Phys. Lett.* 282 (1998) 233–238.
- [18] H.F. Brito, O.L. Malta, J.F.S. Menezes, *J. Alloy Compd.* 303–304 (2000) 336–339.